JOURNAL OF VIROLOGY, Aug. 2007, p. 8247–8257 Vol. 81, No. 15
0022-538X/07/$08.00+0 doi:10.1128/JVI.00312-07

Matrix Fibronectin Binds Gammaretrovirus and Assists in Entry: New Light on Viral Infections▽†

Christiane Beer[1] and Lene Pedersen[1,2]*

Department of Molecular Biology[1] and Institute of Clinical Medicine,[2] Aarhus University, 8000 Aarhus C, Denmark

Received 12 February 2007/Accepted 14 May 2007

A major entry route for the gammaretrovirus amphotropic murine leukemia virus (A-MLV) into NIH 3T3 fibroblasts is via caveola-dependent endocytosis. However, during the infection time, few viral particles can be observed intracellularly. Analyzing the dynamics of the A-MLV infection process by using total internal reflection fluorescence microscopy, we show that the majority of viruses are extracellular and bound to the fibronectin matrix. Moreover, the amounts of bound virus and of fibronectin correlated. Using confocal microscopy, nanoparticles targeted to fibronectin by a III1C-fibronectin fragment or anti-fibronectin antibody were detected intracellularly in NIH 3T3 cells; unconjugated nanoparticles neither bound to cells nor were detectable intracellularly. Furthermore, A-MLV colocalized intracellularly with the fibronectin-targeted nanoparticles, suggesting that they were taken up by the same cellular pathway. Both A-MLV entry and fibronectin turnover depend on caveolar endocytosis, and we found that inhibiting viral binding to the extracellular NIH 3T3 fibronectin-matrix dramatically reduced A-MLV infection, indeed, showing an active role of fibronectin in infection. We suggest that binding to the cellular fibronectin matrix provides a new mechanism by which viruses can enter cells.

Knowledge of the role of cellular factors in retroviral entry increases our understanding of how viruses can exploit cellular features to enter host cells. Gammaretroviruses, like other enveloped viruses, are dependent on specific cellular receptors for fusion of the viral membrane with the cellular membrane; e.g., amphotropic murine leukemia virus (A-MLV) depends on the presence of the ubiquitously expressed sodium-dependent phosphate transporter Pit2 (17, 29, 48, 50). MLV-based retroviral vectors including vectors carrying A-MLV envelope proteins are widely used in gene therapy protocols, and although retroviruses and retroviral vectors can infect a variety of dividing cell types, the efficiencies vary greatly among different cell types despite the fact that these cells all express Pit2 (48). Specifically, efficient transduction of hematopoietic cells can only be achieved when infection occurs in the presence of chymotryptic fibronectin (FN) fragments like 30/35 FN, recombinant chimeric FN fragments like CH-296 (RetroNectin) (13, 32), or shed FN (sFN) derived from NIH 3T3-based packaging cell lines (21 and C. S. Søndergaard, C. Haldrup, C. Beer, D. B. Kohn, and L. Pedersen, submitted for publication). It has been suggested that increased infection is due to concomitant binding of vectors and cells to the fibronectin fragments and that this increases the likelihood that a vector and a cell will interact compared to the situation where both vectors and cells would be in suspension (13, 31). In agreement with this hypothesis, we could recently show that gammaretroviral vectors bind to sFN from NIH 3T3 cultures (Søndergaard et al., submitted). However, the role of naturally occurring FN in viral entry is largely unknown.

FN is a component of the extracellular matrix (ECM) of cells (14) and plays important roles in cell adhesion, migration, proliferation, and differentiation (11, 15). It is produced by a number of cell types including fibroblasts (47, 55) and consists of two nearly identical ~250-kDa subunits, which are covalently linked by disulfide bonds (51). Depending on the species, alternative splicing of a single coding pre-mRNA generates up to 20 FN isoforms (20). These FN isoforms are, based on their solubility, subdivided into soluble plasma FN and less-soluble cellular FN, e.g., ECM FN (reviewed in reference 36). Cell surface FN has been found on various cell lines including fibroblasts (56), astroglial cells (49), and certain cultured epithelial cells (7, 9). Depending on the cell line, cellular FN builds an extensive network and is, moreover, continuously secreted or sloughed from cells into their culture media (9, 49); we refer to FN present in the culture medium as sFN.

The abilities of FN to polymerize and aggregate lead to the formation of characteristic ECM FN fibrils. Formation of FN fibrils and their incorporation into the ECM of cells are tightly regulated processes (24 and reviewed in reference 26) and are mediated through different binding sites, which are localized at several positions within the FN protein. FN polymerization has been shown to be essential for the organization and maintenance of the FN matrix (46). Maintenance of the FN matrix also involves synthesis, deposition, and degradation of FN, and Sottile and Chandler recently found that FN degradation is dependent on caveolin-1, showing that FN turnover occurs through caveolae (45).

Caveolae are omega-shaped cholesterol-rich invaginations of the plasma membrane that play an important role in endocytosis and transcytosis (3) and which also have been reported to be involved in the entry of viruses like simian virus 40 (2, 38), echovirus (27), human polyomavirus BK (10), and human

* Corresponding author. Mailing address: Department of Molecular Biology, Aarhus University, C. F. Møllers Allé, Building 130, DK-8000 Aarhus C, Denmark. Phone: 45-8942-2633. Fax: 45-8619-6500. E-mail: LP@mb.au.dk.

† Supplemental material for this article may be found at http://jvi.asm.org/.

▽ Published ahead of print on 23 May 2007.

coronavirus 229E (34). They were, moreover, shown to be one of several possible entry routes for influenza virus (35). Recently, we showed that retroviruses can also enter cells through caveolae (5), as had previously been indicated from studies of ecotropic MLV (25). Thus, impairing caveolar function severely impaired A-MLV infection of NIH 3T3 cells, and viral particles could be detected intracellularly colocalized with caveolin-1 (5). However, interestingly, compared to the multiplicity of infection employed during these studies, only a few viral particles could be detected intracellularly (5). This observation, together with the fact that gammaretroviruses can bind to FN fragments, led us to investigate the role of ECM FN in the gammaretroviral infection of cells with an FN matrix.

We show here that A-MLV indeed is able to bind to the FN matrix of mouse fibroblasts and that the amount of cell-bound viral particles is dependent on the amount of ECM FN. Furthermore, using fluorescently labeled FN and A-MLV, we were able to show that FN and A-MLV colocalize intracellularly. As the inhibition of binding of A-MLV to FN significantly decreased its infection of mouse fibroblasts, we suggest that binding to the ECM FN of fibroblasts is important for the virus to overcome the ECM and to enter these cells. In addition, based on our results, we propose a new model for A-MLV binding and entry, which may be important for other FN-binding viruses.

MATERIALS AND METHODS

Cells. NIH 3T3 (ATCC CRL-1658), MDTF (a kind gift from Melvyn Yap), and BHK21 (a kind gift from Dagmar Wirth) cells were propagated in Dulbecco's modified Eagle's medium (DMEM) (Gibco BRL) supplemented with 10% newborn calf serum (NCS) (Gibco BRL) and 100 IU/ml penicillin and 100 μg/ml streptomycin (PS) (Gibco BRL). 293T cells (ATCC CRL-11268) were propagated in DMEM supplemented with 10% fetal calf serum (FCS) and PS. Jurkat cells (a kind gift from Steffen Junker) were propagated in RPMI-1640 medium (Gibco BRL) supplemented with 10% FCS and PS. PT67 cells (28) were propagated in DMEM with 10% NCS and PS. All cells were grown at 37°C, 10% CO_2, and 95% humidity.

Conjugation of Qdot nanocrystals. Polyclonal rabbit anti-FN antibody (300 μg; Dako) and 300 μg III1C FN fragment (Sigma) were conjugated to Qdot 655 nanocrystals as described by the manufacturer (Quantum Dot Corporation) and are referred to as anti-FN-Qdot and III1C-Qdot, respectively. The resulting conjugated Qdot-containing solutions were used at 1:200 dilutions for staining of fibronectin and for uptake experiments.

Stable transfection. To stably express a caveolin-1 mRed fusion protein (cav-1 mRed), NIH 3T3 cells were transfected using the calcium phosphate precipitation method with a construct encoding the cav-1 mRed fusion protein (43). The cells were selected in medium containing 731 μg/ml active G418 and thereafter were cultivated without selection.

β-Galactosidase assay of infected cells. The β-galactosidase (β-Gal) assay was performed as described previously (37). The cells were fixed with 0.05% glutaraldehyde, washed with phosphate-buffered saline (PBS), and overlaid with X-Gal (5-bromo-4-chloro-3-indolyl-β-D-galactopyranoside) containing (1 mg/ml) staining solution (5 mM potassium ferricyanate, 5 mM potassium ferrocyanate, 2 mM $MgCl_2$). β-Gal-positive (blue) cells were counted using a light microscope.

Production of infectious and fluorescent noninfectious A-MLV. A construct carrying the Moloney MLV *gag* gene with the yellow fluorescent protein (YFP)-encoding sequence fused to the nucleocapsid-encoding sequence (4) was used for the production of fluorescent noninfectious A-MLV (GagYFP A-MLV). For the production of GagYFP A-MLV particles, 293T cells were seeded in T75 flasks and grown to 70% confluence. The cells were transiently cotransfected with the GagYFP-encoding construct pHIT111 (harboring a β-Gal-encoding transfer vector) (44) and a pHIT-derived vector encoding the A-MLV (4070A isolate) envelope protein. For the production of fluorescent virus particles not carrying an envelope protein (GagYFP no-env), transfection was performed in the same way, except that no A-MLV envelope protein-encoding plasmid was added. Infectious virions carrying A-MLV envelope proteins were produced by transiently cotransfecting 293T cells with a plasmid carrying the Moloney MLV *gag-pol* gene (pHIT60) (44), pHIT111, and the pHIT-derived vector encoding A-MLV envelope protein. The obtained titers were $\sim 1 \times 10^4$ blue forming units/ml.

For all vector types, 48 h after transfection, the supernatants were harvested, filtrated (0.45-μm filter), and stored at −80°C until use.

Estimation of viral particle concentration. GagYFP A-MLV- or GagYFP no-env-containing supernatants were mixed with Polybrene (8 μg/ml), transferred to 8-well chamber slides (LabTek, Nunc), and incubated overnight at 37°C. After being washed with PBS, the particles were fixed to the glass surface using 4% paraformaldehyde (PFA). Samples were analyzed using a model IX70 fluorescence microscope (Olympus) fitted with a model 41001 filter (Chroma) at 1,000× magnification. Images were taken with a Colorview II camera (Olympus). Brightness and contrast were adjusted (Adobe Photoshop).

Anti-FN antibody treatment of cells. NIH 3T3 cells were seeded at 3×10^4 per well in a 24-well plate (Nunc) and grown overnight. Next day, the cells were treated with polyclonal rabbit anti-FN antibody (Dako) (1:50 to 1:1,000 in preheated DMEM/10% NCS). Control cells were treated with DMEM/10% NCS without anti-FN antibody. After 1 h, the cells were infected with A-MLV (8 μg/ml Polybrene) in the presence (1:50 to 1:1,000 dilutions) or absence (control) of anti-FN antibody. Noninternalized viral particles were inactivated 24 h later by using citrate buffer (40 mM sodium citrate, 10 mM KCl, 135 mM NaCl, pH 3.1) (18). The cells were investigated 24 h later for infection events using the β-Gal assay.

Cell growth analysis. NIH 3T3 cells (2×10^5 cells seeded in a T25 cell culture flask [Nunc]) were infected with vectors carrying A-MLV envelope proteins and a β-Gal-encoding transfer vector (a multiplicity of infection of approximately 0.1; 8 μg/ml Polybrene). Infected cells stably express the β-Gal gene. One day later, the cells were transferred into a T75 cell culture flask (Nunc) and cultivated for 3 days. Then, 2×10^4 cells were seeded per well in a 24-well plate and treated for 24 h with different dilutions of polyclonal anti-FN antibody (Dako) (1:50 to 1:1,000 diluted in DMEM/10% NCS) or no antibody as control. Subsequently, the cells were stained for β-Gal expression.

Staining of FN and extracellular colocalization analysis. To stain the extracellular FN matrix, cells were seeded into 8-well chamber slides and grown to ~80% density. In some experiments, the cells were incubated with plasma FN (1 μg/ml; Sigma), CH-296 (1 μg/ml; TaKaRa Bio, Inc.), or PT67 supernatant prior to FN staining. In addition, in some experiments, fluorescent viral particles were added after incubation with FN or PT67 supernatants and prior to staining. After cells were washed with PBS, they were fixed with 4% PFA, and unspecific binding sites were blocked using 3% bovine serum albumin/10% FCS. The cells were subsequently stained for FN, using a polyclonal rabbit anti-FN antibody (Sigma) and phycoerythrin (PE)-conjugated anti-rabbit immunoglobulin G (IgG) from goat (Sigma). Samples were analyzed using a fluorescence microscope (IX70; Olympus; with filter sets for YFP, 41001, and for PE, U-MWIG; Chroma) at 1,000× magnification. Images were taken with a Colorview II camera (Olympus). Brightness and contrast were adjusted (Adobe Photoshop).

Alternatively, FN was stained using anti-FN-Qdot. Confocal images were captured with a Leica TCS SP confocal microscope (oil immersion HCX PlanApo CS ×40 objective, numerical aperture [NA] 1.25 objective) (Leitz). YFP and Qdot 655 nanocrystals were excited using an argon laser 488-nm line. The two single-color images were subsequently merged into a red-green-blue image.

Three-dimensional confocal microscopy for analysis of intracellular colocalization. To investigate the uptake of anti-FN-Qdots or III1C-Qdots, NIH 3T3 cells were incubated with anti-FN-Qdot crystals (12 h) or III1C-Qdot crystals (5 or 24 h). In some experiments, anti-FN-Qdots or III1C-Qdots were mixed with GagYFP A-MLV and added to the cells in the presence of 8 μg/ml Polybrene. As control, unconjugated Qdot 655 nanocrystals (1:200 diluted in DMEM/10%FCS with 8 μg/ml Polybrene) were used. After cells were washed with PBS, they were fixed with 4% PFA, and confocal image stacks were captured with a Leica TCS SP confocal microscope (pinhole 1.0 airy-disk units; oil immersion HCX PlanApo CS ×40 objective, NA 1.25) (Leitz). YFP and Qdot 655 nanocrystals were excited using an argon laser 488-nm line. Image stacks were processed using ImageJ (version 1.34) (1).

Live-cell imaging. NIH 3T3 cells stably expressing cav-1 mRed were seeded on chamber slides 1 day prior to the experiments. The cells were incubated for 1 h with GagYFP A-MLV in the presence of 8 μg/ml Polybrene, washed twice with prewarmed medium, and immediately used for total internal reflection fluorescence microscopy (TIRFM). Images were taken using an Olympus IX70 microscope (oil immersion PlanApo ×60 objective, NA 1.45 TIRFM; Olympus) at 5-s time intervals with 210-ms exposure times and 1-by-1 binning. The microscope was controlled by Cell-R software (Olympus BioSystems [now OSIS], Germany) and fitted with an MT20 light source, solid-state diode lasers, a condenser

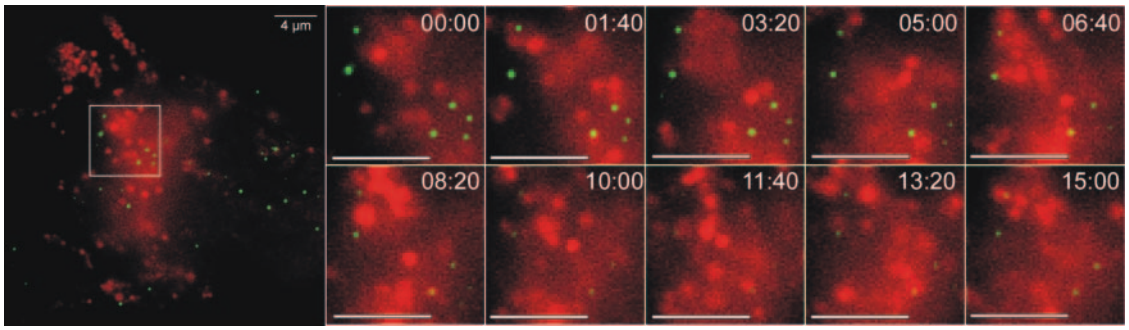

FIG. 1. Live-cell imaging of cav-1 mRed-expressing NIH 3T3 cells exposed to GagYFP A-MLV, using live-cell TIRF microscopy. The left panel shows the first frame taken. The panels on the right are enlarged images of the area indicated by the square, taken from the video sequence (180 frames, time is shown in min:s). Caveolin-1 mRed is shown in red, and GagYFP A-MLV is shown in green. See Video S1 in the supplemental material.

coupling for objective type TIRF illumination, and a cooled "F-View" charge-coupled device camera. GagYFP A-MLV was excited at 488 nm and cav-1 mRed at 532 nm. Images and movies were processed using ImageJ (version 1.34) (1).

Flow cytometry. Adherent cell lines were detached using EDTA buffer (1 mM EDTA in PBS), and 5×10^5 cells were fixed (1% PFA) and stained for FN by using 1 μg rabbit anti-FN antibody (Sigma) and PE-conjugated anti-rabbit IgG. Negative controls were mock treated (virus binding experiments) or treated only with PE-conjugated antibody. In some experiments, the cells were incubated with 1 μg/ml plasma FN, 1 μg/ml CH-296, PT67 supernatant, GagYFP A-MLV, or GagYFP no-env at 37°C prior to fixation and FN staining. Finally, the cells were passed through 35-μm filters (Falcon) and analyzed using a FACSCalibur (BD). Data were analyzed using CellQuest software (BD).

Statistical analysis. The hypothesis that two mean values were identical was tested by a two-tailed Student's *t* test; values were considered different at a 95% confidence level.

RESULTS

The majority of A-MLV virions are immobilized extracellularly after their addition to NIH 3T3 cells. A major entry route for the gammaretrovirus A-MLV into NIH 3T3 mouse fibroblasts is via caveola-dependent endocytosis; however, compared to the multiplicities of infection employed, few viral particles were observed intracellularly (5). To analyze the dynamics of the A-MLV infection process, we used TIRF microscopy, which allows for the investigation of viral particles and caveolae at or near the cell surface. The A-MLV particles used were produced by transient transfection of 293T cells and carried a viral nucleocapsid protein fused to YFP (GagYFP A-MLV), which renders the vectors fluorescent and fusion defective (4). Fluorescent A-MLVs were added to NIH 3T3 cells stably transfected with cav-1 mRed, and the cultures were incubated at 37°C for 1 h before unbound viral particles were removed and cells were analyzed by TIRF microscopy. Only a small amount of the viral particles was found associated or colocalized with caveolin-1 (5), in agreement with our previous studies; however, the noncolocalized viruses remained at the cell surface, with only minimal or without any movement (Fig. 1 and see Video S1 in the supplemental material). The disappearance of the viral particles was most likely due to bleaching and not the result of uptake by the cells. Studying vectors produced by NIH 3T3-derived packaging cell cultures, we recently found that gammaretroviral vectors can bind to sFN fragments (Søndergaard et al., submitted), and we therefore speculated that the A-MLV particles, after addition to NIH

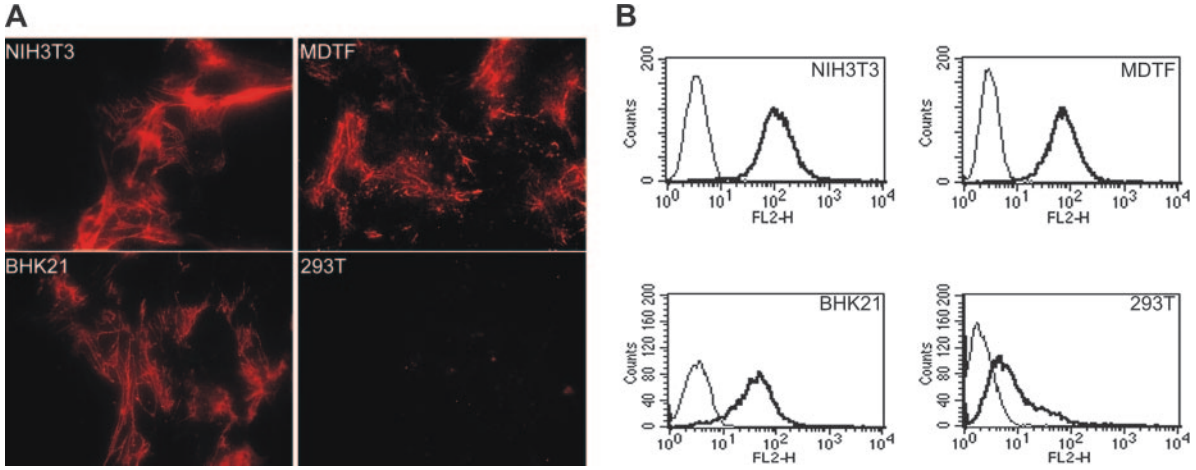

FIG. 2. Characterization of FN expression. (A) Immunocytochemical staining of ECM FN on fixed cells of the indicated cell lines using anti-FN antibody and PE-conjugated secondary antibody demonstrates differences in the appearance of ECM FN (red). Pictures were taken using a fluorescence microscope and an oil immersion objective (original magnification, ×1,000). (B) Characterization of FN expression of indicated cell lines using flow cytometry. Cells were detached, and equal amounts of cells were incubated with anti-FN antibody and PE-conjugated secondary antibody. Thin line indicates cells incubated with secondary antibody only; thick line indicates cells incubated with primary and secondary antibodies.

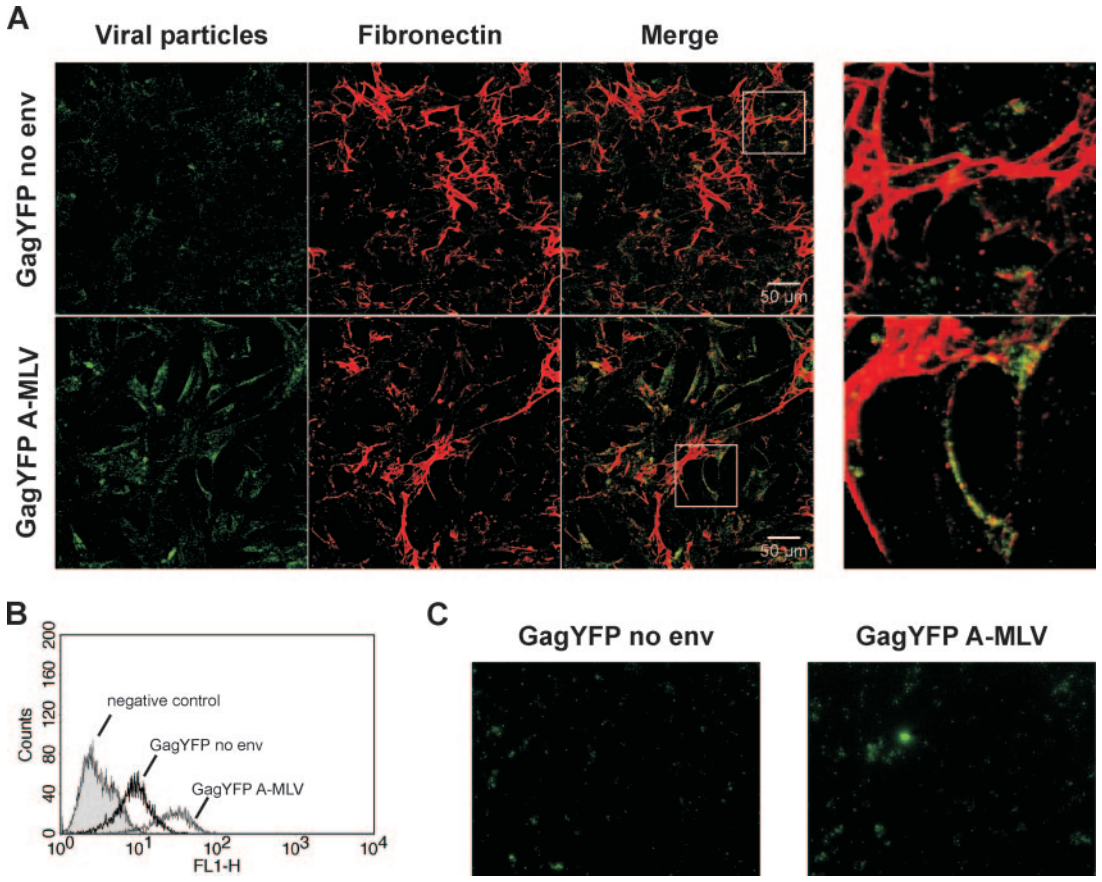

FIG. 3. (A) Colocalization of GagYFP A-MLV and GagYFP no-env particles with ECM FN of NIH 3T3 cells. GagYFP A-MLV and GagYFP no-env particles were incubated for 12 h with NIH 3T3 cells, and the cultures were fixed and stained for ECM FN using anti-FN-Qdots. GagYFP particles are shown in green, and ECM FN is shown in red; colocalization results in yellow signals. Panels at the right are enlargements of the areas within the squares indicated in the merged images. Images were taken using confocal microscopy (original magnification, ×400). (B) Flow cytometry analysis of GagYFP A-MLV and GagYFP no-env binding to NIH 3T3 cells. Mock-treated NIH 3T3 cells are shown as the gray-shaded trace. (C) Estimation of the amounts of GagYFP A-MLV and GagYFP no-env particles. Equal amounts of particle-containing supernatants were loaded onto chamber slides and examined using a fluorescence microscope. Pictures were taken randomly with an oil immersion objective (original magnification, ×1,000).

3T3 cell cultures, might be immobilized by binding to the ECM FN of these cultures.

NIH 3T3 cells have a pronounced FN matrix to which viral particles adhere. To visualize the structure of the ECM FN of NIH 3T3 cells, cells were seeded in chamber slides, fixed, stained for FN using an anti-FN antibody, and examined by fluorescence microscopy. For comparison, *Mus dunni* tail fibroblasts (MDTF), baby hamster kidney fibroblasts (BHK21), and human embryonic kidney cells (293T) were analyzed in parallel. As expected, FN fibrils were present in cultures of the fibroblastic lines NIH 3T3, MDTF, and BHK21. The FN fibrils of MDTF cells were noticeably shorter than those of NIH 3T3 and BHK21 cells (Fig. 2A). In comparison, 293T cells showed only minimal staining for FN, and no FN fibrils were observed (Fig. 2A). The microscopy data shown in Fig. 2A were confirmed by flow cytometry (Fig. 2B). Thus, NIH 3T3 cells possess extensive ECM FN, and using immunocytochemical staining, we investigated whether A-MLV did bind to this matrix. For comparison, fluorescent GagYFP no-env viral particles were included; these were made as described for the GagYFP A-MLV particles, except that no A-MLV envelope-encoding plasmid was included in the transient transfection (Fig. 3C). NIH 3T3 cells were seeded into chamber slides and incubated with GagYFP A-MLV or GagYFP no-env particles, fixed, and stained for ECM FN (Fig. 3A). Large amounts of fluorescent GagYFP A-MLV particles were found to bind to FN fibrils in the ECM (Fig. 3A), which can explain why the majority of the viruses shown in Fig. 1 remained immobilized. Interestingly, GagYFP no-env particles also partially colocalized with FN (Fig. 3A) and bound to NIH 3T3 cells (Fig. 3B). The smaller amount of envelope-protein-free particles bound to FN and NIH 3T3 cells compared to that of GagYFP A-MLV particles (Fig. 3A and B) is most likely due to a lower concentration of envelope-protein-free vector particles (Fig. 3C). Therefore, we suggest that the A-MLV envelope protein is not essential for the attachment of A-MLV particles to NIH 3T3 cells and ECM FN.

A-MLV binding to cell lines correlates with the amount of their attached FN. If the FN matrix of cells is important for binding of A-MLV, cell lines expressing smaller amounts of FN might be expected to bind smaller amounts of viral particles. To address this, equal numbers of NIH 3T3, MDTF,

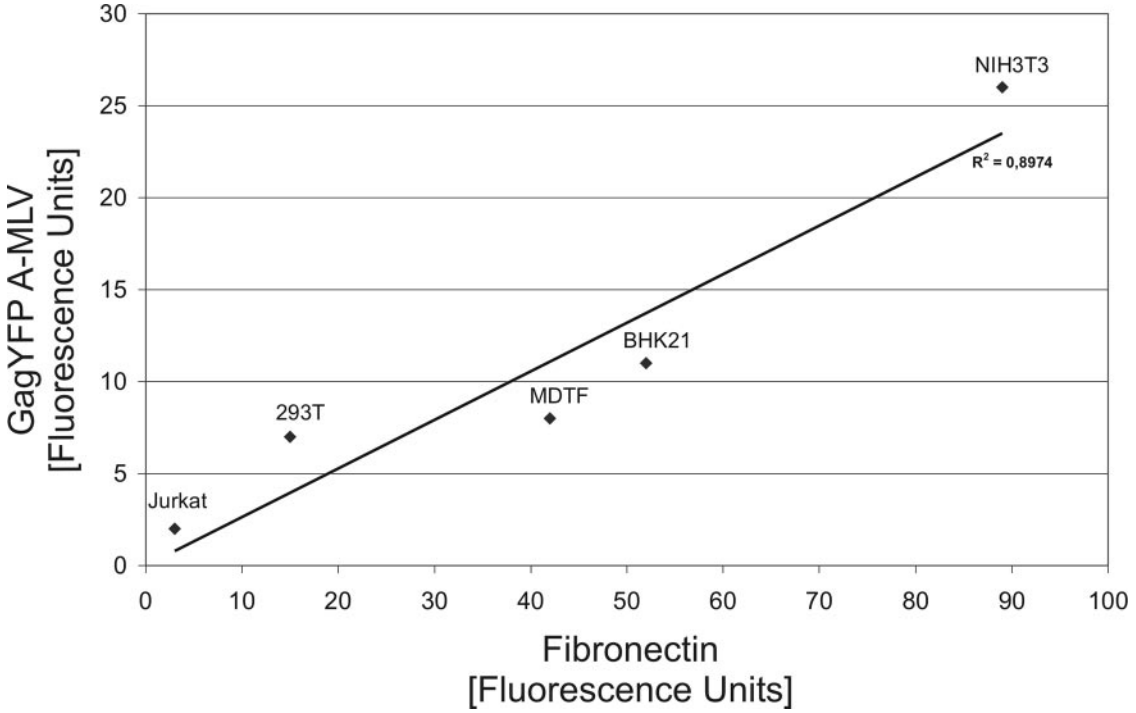

FIG. 4. Amount of bound GagYFP A-MLV particles correlates with the amount of bound ECM FN. GagYFP A-MLV was incubated with 5×10^5 cells of the indicated lines for 1 h at 37°C. Fixed cells were incubated with anti-FN antibody and secondary PE-conjugated antibody, and the amounts of bound virus and ECM FN were analyzed by flow cytometry. The measured fluorescence units (corrected by subtracting background values) were used to correlate the virus binding to the amounts of cell-associated FN. Shown is one typical result out of three independent experiments.

BHK21, 293T, and the human T-cell line Jurkat were incubated with GagYFP A-MLV and analyzed by flow cytometry for FN and bound GagYFP A-MLV (Fig. 4). Small amounts of FN corresponded to lower binding of GagYFP A-MLV and vice versa (Fig. 4), indicating that there is a correlation between the amount of FN associated with the cells and the binding of A-MLV.

NIH 3T3-derived sFN is built into the ECM of fibroblasts. As mentioned above, we recently found that NIH 3T3-derived gammaretroviral vector packaging cells produce sFN of various sizes and that vector particles were bound to the sFN fragments (Søndergaard et al., submitted). The sFN-bound vectors can infect NIH 3T3 and MDTF cells, which we found intriguing since both cell types have extensive FN matrices. We therefore investigated the fate of the packaging cell-derived sFN after its addition to NIH 3T3 and MDTF cells. For that purpose, we used supernatant produced by the PT67 packaging cell, which we found to be the highest sFN producer among the packaging cell lines previously analyzed, amounting to approximately 0.1 μg/ml sFN (Søndergaard et al., submitted). NIH 3T3 and MDTF cells and 293T cells as control were incubated with PT67 supernatant and stained for FN (Fig. 5A). As soon as 1 h after incubation with PT67 supernatant, the FN fibrils in the NIH 3T3 and MDTF cultures became longer and even more pronounced. Moreover, flow cytometry analyses showed increased amounts of FN associated with cells which had been exposed to PT67 supernatant (Fig. 5B). Thus, the PT67-derived sFN was built into the ECM FN of the two fibroblastic lines. Interestingly, 293T cells used sFN from PT67 cells to build up short FN fibrils (Fig. 5A), thus gaining an ECM of FN. The increase in 293T-associated FN after the addition of PT67 supernatant was confirmed by flow cytometry (Fig. 5B). Flow cytometric analysis of the human T-cell line Jurkat showed results similar to those of 293T (Fig. 5C).

Next, we investigated whether the increase in FN matrix of NIH 3T3 cells caused by the PT67-derived sFN increased the binding capacity for A-MLV. NIH 3T3 cells were seeded on chamber slides and incubated with PT67 supernatant, plasma FN, or the FN fragment CH-296. Subsequently, the cells were incubated with GagYFP A-MLV, fixed, and stained for FN (Fig. 5D). Incubation with PT67 supernatant led to increased FN matrix staining, as shown in Fig. 5A, whereas incubation with plasma FN or CH-296 had no effect (Fig. 5D), even though 10-fold higher concentrations were applied in the latter two cases. Moreover, the presence of sFN from PT67 cells did increase the level of cell-bound GagYFP A-MLV, while plasma FN or CH-296 had no effect. Using a higher magnification, Fig. 5E shows that GagYFP A-MLV particles bound to FN fibrils present on NIH 3T3 cells after incubation with PT67 supernatant. The correlation between the increased FN amounts and the numbers of bound viruses is in agreement with the observations shown in Fig. 4.

A-MLV colocalizes intracellularly with the labeled III1C FN fragment. The immobilization of the viral particles on the NIH 3T3 ECM FN identified here was intriguing, since we recently found that A-MLV mostly enters NIH 3T3 cells through caveola-dependent endocytosis (5). However, in 2005, Sottile and Chandler reported that FN turnover also occurs via caveo-

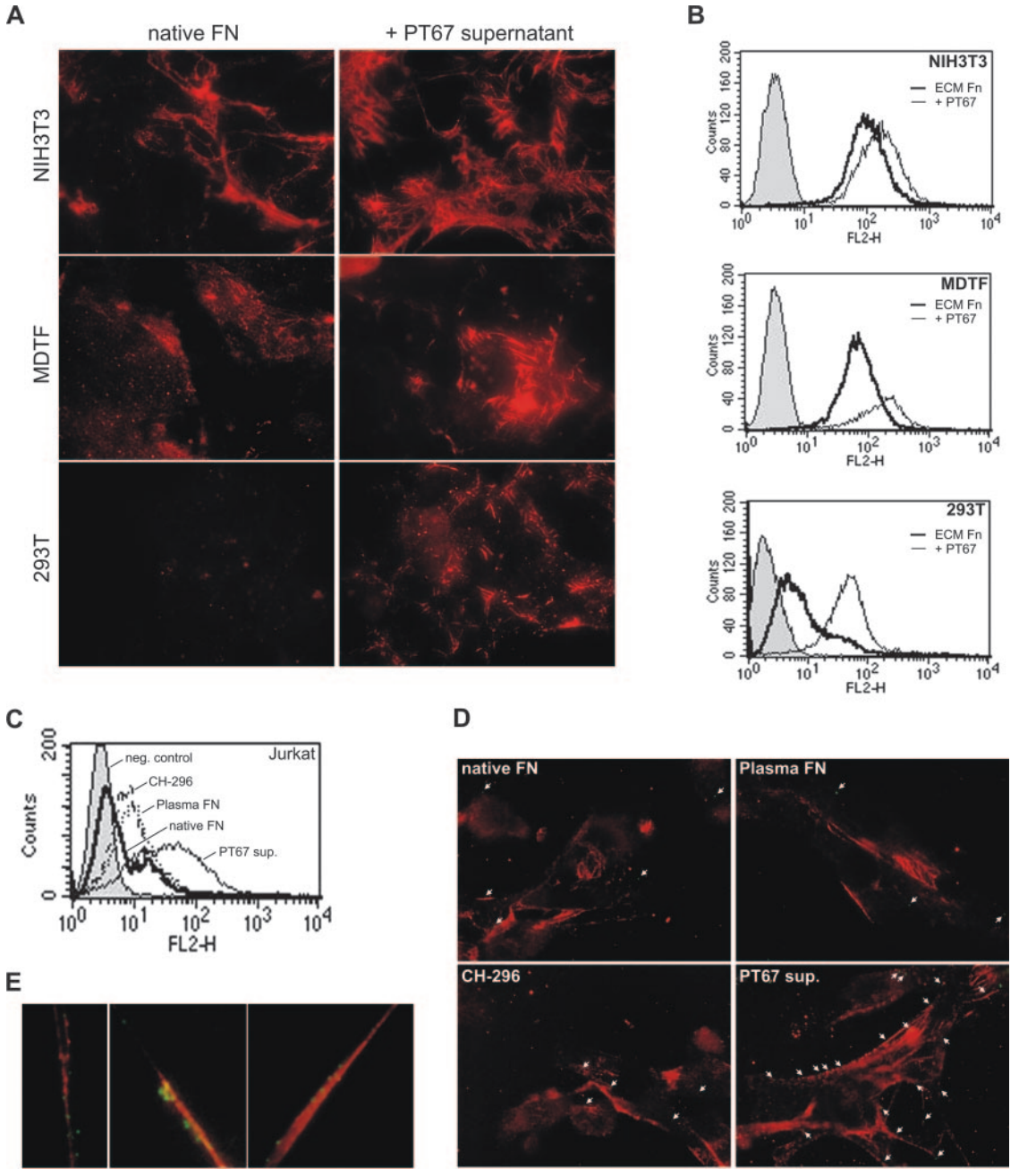

FIG. 5. (A) Immunocytochemical staining of binding of PT67-derived sFN to cells. The cells were incubated for 1 h with fresh cell culture medium or PT67 supernatant (~ 0.1 μg/ml FN), fixed, and stained for FN as shown in Fig. 2A. Pictures were obtained using a fluorescence microscope (original magnification, ×1,000). (B) sFN from fibroblasts binds to cells. Equal numbers of the indicated cells were incubated for 1 h at 37°C with normal cell culture medium or with PT67 supernatant (~ 0.1 μg/ml FN), stained for FN using an anti-FN antibody and PE-conjugated secondary antibody, and analyzed using flow cytometry. Gray-shaded trace, negative control (stained only with secondary antibody); thick line, fresh medium added; thin line, cells incubated with PT67 supernatant. (C) Flow cytometry analysis of FN binding to Jurkat cells. The cells were incubated for 75 min at 37°C with normal cell culture medium, plasma FN, FN fragment CH-296, or PT67 supernatant and subsequently stained and examined for cell-bound FN as described in panel B legend. (D) Increased GagYFP A-MLV binding to NIH 3T3 cells after treatment with PT67 supernatant. Immunocytochemical staining of NIH 3T3 cells incubated with fresh cell culture medium or equal volumes of plasma FN (1 μg/ml), CH-296 (1 μg/ml), or PT67 supernatant (~ 0.1 μg/ml FN) for 1 h at 37°C, followed by 2 h of incubation with GagYFP A-MLV. Cells were fixed and stained for FN as shown in Fig. 2A. GagYFP particles are shown in green; ECM FN is shown in red. White arrows point at GagYFP particles. Pictures were obtained with a fluorescence microscope (original magnification, ×1,000). (E) GagYFP A-MLV bound to ECM FN of NIH 3T3 cells treated with PT67 supernatant (see panel D legend).

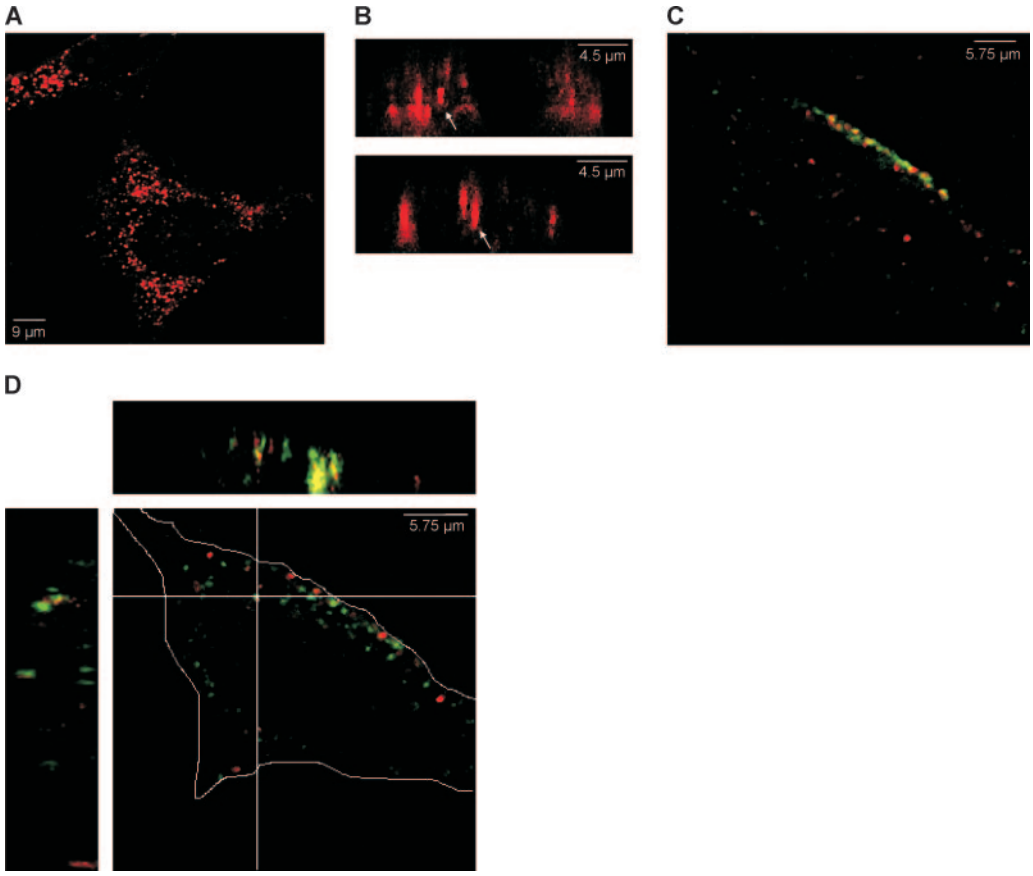

FIG. 6. Localization of III1C-Qdots and GagYFP A-MLV after addition to NIH 3T3 cells. (A and B) NIH 3T3 cells were incubated with III1C-Qdots (red) for 24 h at 37°C, fixed, and subsequently examined by confocal microscopy. (B) Cells were examined using 3D scanning confocal microscopy (44 slices; 0.20-μm spacing). Shown are two examples of a *Y-Z* section showing intracellular localization of III1C-Qdots (arrows). (C) Colocalization of III1C-Qdots with GagYFP A-MLV at the cell surface. NIH 3T3 cells were incubated with III1C-Qdots (red) and GagYFP A-MLV (green) for 5 h at 37°C, fixed, and subsequently examined by confocal microscopy. Colocalization resulted in the yellow color. (D) NIH 3T3 cells were incubated with III1C-Qdots (red) and GagYFP A-MLV (green) for 5 h at 37°C, fixed, and subsequently examined for the presence of intracellular colocalization of GagYFP A-MLV and III1C-Qdots (yellow) using 3D scanning confocal microscopy (25 slices; 0.38-μm spacing). Shown are the *Y-Z* (left) and *X-Z* (top) sections with the corresponding *X-Y* section. The contour of the cell is shown with a line.

lae (45). These three observations together led us to hypothesize that binding of A-MLV to FN may result in cellular uptake of FN-bound viral particles through caveola-mediated endocytosis. To address this hypothesis, 10-nm fluorescent nanocrystals (Qdots) were conjugated with the 76-amino-acid FN fragment III1C, representing the first type III module of FN (III1C-Qdots). The III1C fragment is known to be incorporated into the FN matrix of cells, and moreover, the cultivation of cells with III1C does not cause a loss of FN matrix (19). To investigate whether III1C-Qdots are taken up by NIH 3T3 cells, cells were seeded in chamber slides and incubated with III1C-Qdots for 24 h. Three-dimensional (3D) confocal microscopy revealed a mainly dot-like staining of the cells (Fig. 6A), while FN fibrils were only negligibly stained. Moreover, intracellular III1C-Qdots were detected (Fig. 6B), indicating that III1C-Qdots were taken up by NIH 3T3 cells. Unconjugated Qdots neither bound in significant amounts to NIH 3T3 cells nor could they be detected intracellularly (data not shown). Thus, the 10-nm Qdots conjugated with III1C can be taken up by NIH 3T3 cells.

To investigate whether A-MLV colocalized with III1C-Qdots, NIH 3T3 cells were incubated with III1C-Qdots and GagYFP A-MLV for 5 h. 3D confocal microscopy revealed that GagYFP A-MLV not only colocalized with III1C-Qdots extracellularly (Fig. 6C) but also intracellularly (Fig. 6D). These results suggest that FN-bound A-MLV can be taken up together with the Qdot-labeled FN III1C fragments.

A large part of intracellular A-MLV directly colocalizes with anti-FN stained ECM FN. To directly investigate whether ECM FN with ligand, e.g., Qdots or A-MLV, is taken up by NIH 3T3 cells, we used GagYFP A-MLV and Qdots conjugated with anti-FN antibody (anti-FN-Qdots) to label FN. Unlike the III1C FN fragment, anti-FN antibodies are known to influence the extracellular FN matrix and to lead to redistribution of FN into large aggregates (53). In agreement with this, we also found reorganization of the ECM FN when incubating NIH 3T3 cells for 24 h with anti-FN antibody (data not shown). To investigate whether FN-bound A-MLV was taken up by the cells and colocalized intracellularly with anti-FN-Qdots, NIH 3T3 cells were incubated for 12 h with GagYFP A-MLV and anti-FN-Qdots. Using 3D confocal microscopy, we could indeed show that a large part of the GagYFP A-MLV particles

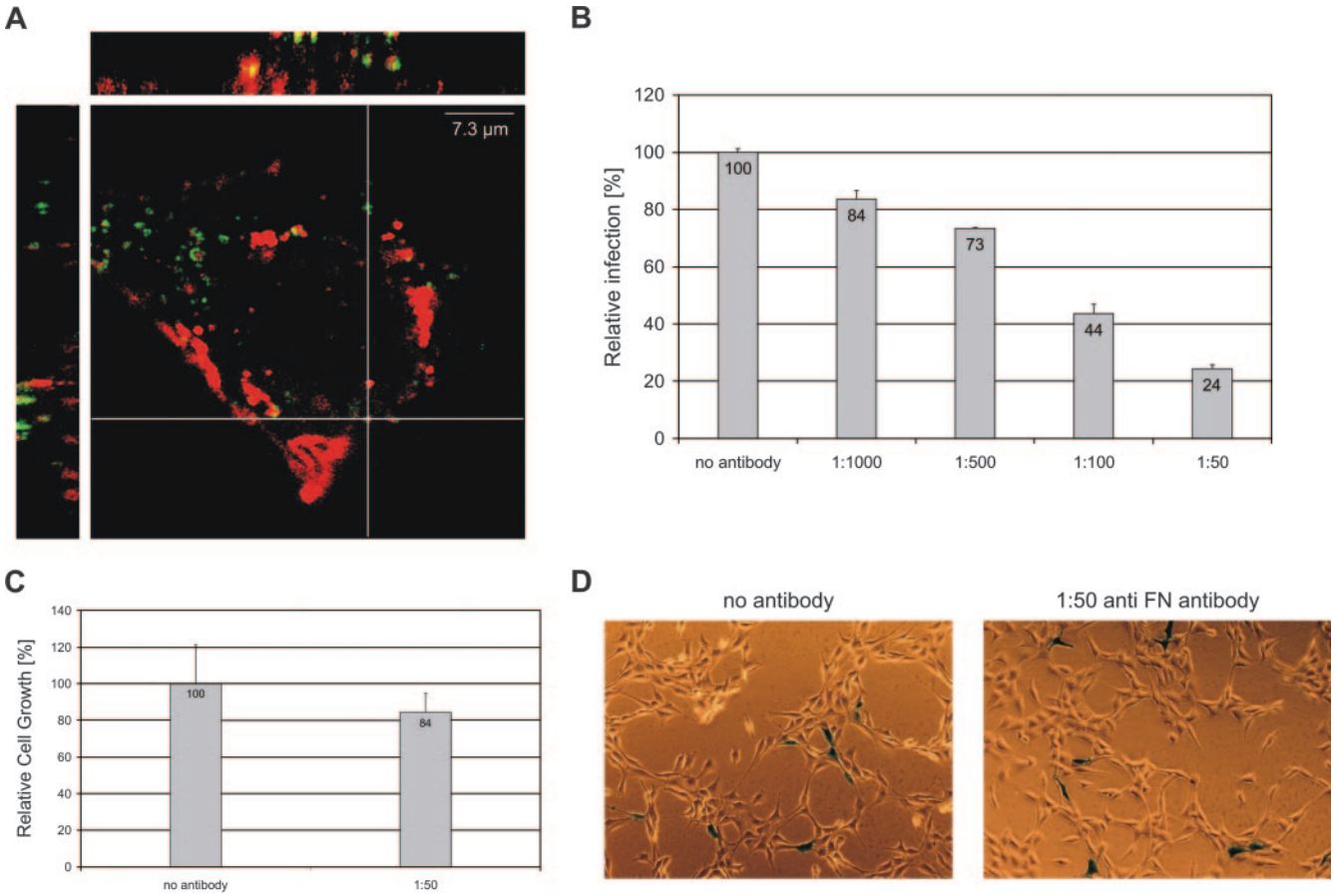

FIG. 7. Analysis of the role of ECM FN in A-MLV entry of NIH 3T3 cells. (A) Intracellular colocalization of Qdots conjugated to anti-FN antibody with GagYFP A-MLV. NIH 3T3 cells were incubated for 12 h with anti-FN-Qdots (red) and GagYFP A-MLV (green). Fixed cells were examined for the presence of intracellular colocalization of GagYFP A-MLV and anti-FN-Qdots (yellow) using 3D laser scanning confocal microscopy (30 slices; 0.39-μm spacing). Shown are the *Y-Z* (left) and *X-Z* (top) sections with the corresponding *X-Y* section. (B) Inhibition of A-MLV binding to FN decreases viral infection. NIH 3T3 cells were treated with the indicated amounts of anti-FN antibody for 1 h and thereafter were infected with A-MLV (multiplicity of infection, approximately 0.07) in the presence of anti-FN antibody. The numbers of infected cells are normalized to the mock values. Shown are the means ± standard deviations of one experiment done in duplicate. Similar results were obtained with two other independent experiments. (C) Investigation of the effect of anti-FN antibody treatment on the growth of NIH 3T3 cells. NIH 3T3 cells (~5 to 10% β-Gal-positive) were treated with anti-FN antibody or mock treated for 24 h, and β-Gal-positive cells were counted. The numbers of β-Gal-positive cells are normalized to the mock values. Shown are the means ± standard deviations of one experiment done in sextuple. (D) Images of cells from C were obtained by using an IX70 Olympus microscope (original magnification, ×200).

colocalized intracellularly with anti-FN-Qdots (Fig. 7A), strongly suggesting that A-MLV particles bound to FN are taken up by the same pathway as Qdot-labeled FN-bound antibodies.

Preincubation of NIH 3T3 cells with anti-FN antibodies impairs A-MLV infection. If binding to ECM FN of NIH 3T3 cells indeed plays an important role in A-MLV infection, inhibition of viral binding to the extracellular FN matrix should lead to a decrease in A-MLV infection. Therefore, we pretreated NIH 3T3 cells for 1 h with anti-FN antibody to inhibit A-MLV binding to FN. Subsequently, the cells were incubated with infectious A-MLV in the presence of anti-FN antibody. After 24 h, noninternalized viruses were inactivated using citrate buffer, and the cells were incubated for an additional 24 h in normal cell culture medium. As shown in Fig. 7B, depending on the antibody concentration, A-MLV infection was inhibited by up to 76% (for all concentrations, P was <0.05 compared to that of the control).

Infection of cells with A-MLV is dependent on mitosis, and to ensure that the decreased A-MLV infection rate was not due to an affected cell cycle, we also investigated the effect of anti-FN antibody treatment on cell division. NIH 3T3 cells, of which 5 to 10% expressed β-Gal, were mock treated or treated with anti-FN antibody for 24 h and analyzed for β-Gal expression. The differences in the numbers of β-Gal-positive cells were used as measures of the influence of anti-FN antibody treatment on cell division. As shown in Fig. 7C, treatment with anti-FN antibody decreased the amount of β-Gal-positive cells by approximately 16% ($P > 0.2$). This reduction in cell division cannot explain the clearly larger decrease in viral infection. In addition, the antibody-treated cells appeared normal and showed no tendency to detach (Fig. 7D). These data demonstrate that the observed reduction in A-MLV infection by preincubating NIH 3T3 cells with anti-FN antibodies was not due to an impaired cell division but most likely due to impaired viral binding to FN.

In summary, our data strongly suggest that binding to ECM FN is an important step in A-MLV infection of mouse fibroblasts and that this binding can ensure the uptake of viral particles into cells having an FN matrix.

DISCUSSION

Using NIH 3T3 as target cells, we have demonstrated here for the first time that A-MLV binds to ECM FN fibrils. Early studies have shown that FN is relatively immobile compared to other membrane-associated proteins (42). Furthermore, it has been suggested that ECM FN might inhibit the mobility of other components of the cell surface (54). Thus, our finding that A-MLV binds to ECM FN is also in agreement with our observation that cell-attached A-MLV rarely moves. It can also explain our previous finding that during the infection time, few virus particles can be detected intracellularly (5) as the majority of A-MLV seems associated with the rather immobile FN fibrils of the ECM.

Binding to FN did not in general depend on the presence of the A-MLV envelope protein, in that viral particles without envelope proteins also were able to bind to the ECM FN of NIH 3T3 cells. Although, the binding of envelope protein-free particles seemed to be less specific compared to that of particles carrying the A-MLV envelope protein, this could be due to a lower concentration of envelope protein-free vector particles. It has previously been shown that envelope protein-free viral particles can bind to cells (40, 52).

While this is the first time gammaretroviral binding to ECM FN has been shown, other studies have shown that precoating culture plates with the fibronectin fragment CH-296 or other FN fragments leads to increased retroviral infection and that retroviral vectors can bind to these FN fragments (6, 13, 23, 32 and Søndergaard et al., submitted). Specifically, it was shown that A-MLV can bind to plates coated with FN fragment CH-296 via virus-associated heparan sulfate (23); moreover, A-MLV binding to NIH 3T3 cultures was found to be impaired by preincubating the cells with heparin (52). Thus, it is likely that A-MLV binds to ECM FN in the same manner. It cannot be excluded, however, that the virus also can bind via other mechanisms. Such an alternative indirect manner of virus binding to ECM FN indeed seems to exist for viruses associated with FN shed by some virus producer cells. We have thus found that gammaretroviral vectors produced by cultures of the NIH 3T3-based packaging cell line PT67 bind to sFN fragments shed by these cells and that other NIH 3T3-derived packaging cells also produce sFN (Søndergaard et al., submitted). Based on the observation in the present study that sFN produced by PT67 cell cultures can be incorporated into the existing FN matrix of NIH 3T3 and MDTF cells, we suggest an uptake mechanism similar to that of vectors directly associated with the ECM FN. It should be noticed that since vectors without envelope protein also attached to ECM FN, at least one virus-associated molecule involved in binding to the FN matrix is not the envelope protein or envelope protein associated.

Importantly, we also showed here that ECM FN did not merely immobilize A-MLV virions extracellularly by binding these but that the ECM FN was important for efficient infection of NIH 3T3 cells. Indeed, viral particles could be found intracellularly colocalized with anti-FN antibodies. FN matrix turnover occurs via a caveola-dependent process (45), and given that caveola-dependent endocytosis is the major entry route for A-MLV into NIH 3T3 cells and therefore an efficient infection route for the virus in these cells (5), we suggest that A-MLV can be endocytosed in caveolae while sitting on FN. Based on the efficient down-regulation of A-MLV entry with preincubation with anti-FN antibodies, we moreover suggest that FN-assisted entry is a major entry route into NIH 3T3 cells. Indeed, this entry mechanism can explain how the viruses can overcome the extensive ECM of the fibroblastic cells.

Based on the data presented here, we suggest a new entry model for A-MLV infection of cells possessing an FN matrix (Fig. 8). According to this model, binding of A-MLV to ECM FN occurs through virus-associated heparan sulfate or virus-associated sFN. After this first attachment, the viral particles are transported to caveolae. This could occur while the virus is still associated with FN and the FN matrix undergoes its natural turnover process via caveolae. Alternatively, the virus binds to its receptor Pit2 at the cell surface and is transported to caveolae. Presently, we have no results that can directly suggest which route, if any, is favored. But since we previously have found that Pit2 is partly localized in caveolae as well as directly associated with caveolin-1 (5), we suggest that the virus-receptor interaction does not necessarily have to occur at the cell surface; rather, the direction of an FN-bound virus toward caveolae and its uptake into caveolae would be sufficient to provide a microenvironment allowing for an interaction with its receptor.

It is noteworthy that short FN fibrils and a readily evident FN matrix could be seen in 293T cell cultures incubated with PT67 supernatant; however, the role of this process in A-MLV infection is presently not known. Remarkably, when incubating cells with FN fragment CH-296 or commercially available plasma FN, no obvious difference in the appearance of the FN fibrils could be noticed by immunocytochemical staining, although a slight increase in cell-bound FN was found by flow cytometry (Fig. 5C and D and data not shown). As CH-296 is known to allow binding of cells to culture plates (13), its low incorporation into the FN matrix was unexpected. But it is possible that the sFN produced by NIH 3T3 cells but not CH-296 exists in a form allowing for a fast and effective incorporation into the existing ECM FN. However, results by us and others strongly suggest that, like CH-296, sFN can increase gene transfer to different cell types (21 and Søndergaard et al., submitted). Thus, the present observations suggest that the mechanisms behind the abilities of CH-296 and NIH 3T3-derived sFN to increase retroviral gene transfer indeed might differ.

In our studies of A-MLV binding to FN, we included characterization of the ECM FN of different cell lines including the fibroblast lines NIH 3T3, MDTF, and BHK21, as well as the embryonic kidney cell line 293T. As expected, the fibroblast cell lines exhibited a pronounced FN matrix, whereas no FN matrix could be observed with 293T cultures. The data presented here suggest that characterization of the FN matrix is of importance when interpreting virus-cell binding studies and in particular when creating retroviral vectors targeting specific cell types for gene therapy applications. Binding of viruses to cells that do not possess an FN matrix is expected to differ from binding to cells possessing an FN matrix, in that in the latter

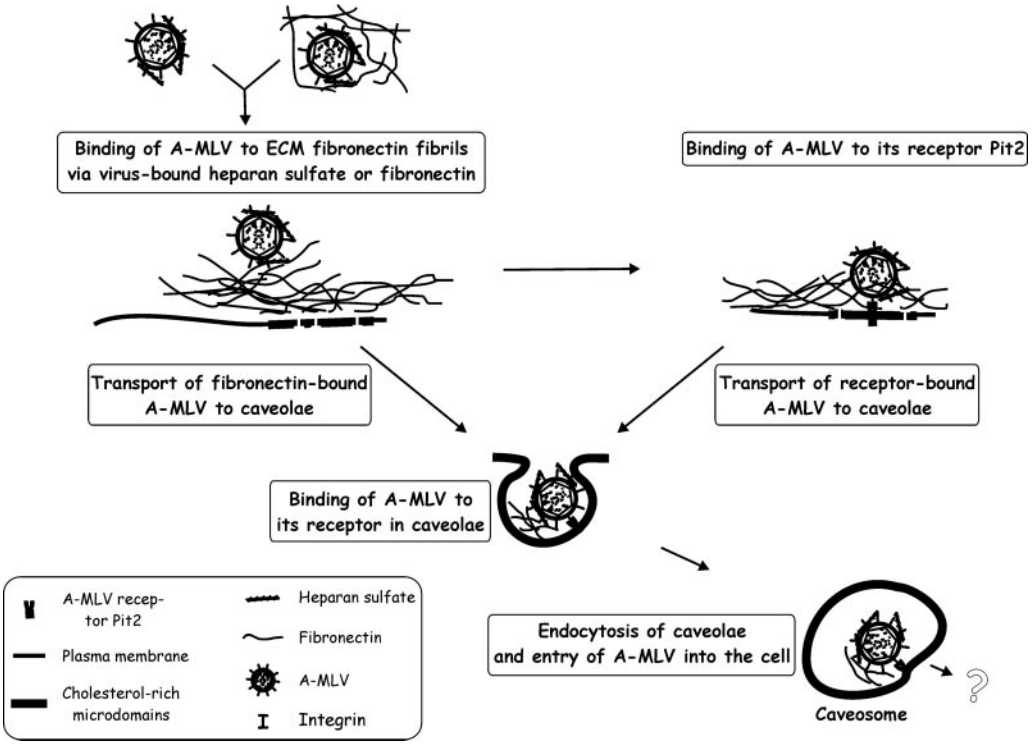

FIG. 8. Model for the early entry steps of A-MLV into cells possessing an FN matrix. See text for details.

situation, our data strongly suggest that viruses able to bind to FN most likely will be immobilized at the ECM FN, which would not only affect their movement at the cell surface but probably also their entry kinetics and infectious half-lives. For human immunodeficiency virus type 1 (HIV-1), it has been shown that incubation with superfibronectin, an in vitro synthesized multimeric form of FN (33), significantly prolonged the infectivity of HIV-1 at 37°C (12). Also for HIV-1, the ECM of cells has therefore been suggested to have a great impact on infections by trapping and stabilizing the viral particles (12). The same may indeed be true for other viruses that are able to bind to FN. In addition, as suggested above, binding of retroviruses to ECM FN might be an important mechanism by which they can overcome the ECM and infect cells. Moreover, as the inhibition of binding to FN significantly reduced A-MLV infection of NIH 3T3 cells, our data also suggest that the FN matrix could protect cells against efficient infection with viruses that are not able to bind to FN.

Binding to FN is not a phenomenon restricted to retroviruses. It has been shown that the envelope protein of influenza A binds to FN (16). Interestingly, Nunes-Correia et al. reported that entry via caveolae is an additional entry route for influenza virus (35). Therefore, our proposed model for A-MLV entry into cells possessing an FN matrix could be applicable to other FN-binding viruses, which may also exploit FN turnover to be taken up by cells. Moreover, FN binding has been shown to play an important role in bacterial infections, e.g., for *Staphylococcus aureus* (22, 39) and *Streptococcus pyogenes* (8). Interestingly, entry of *S. pyogenes* has been related to caveola-dependent endocytosis; indeed, it seems to be the major entry route for *S. pyogenes* (41). In addition, it has been shown that beads coated with the FN-binding protein Sfbl of *S. pyogenes* are efficiently taken up by cells (30, 41). Therefore, we suggest that binding to FN might be a general mechanism for transport of FN-bound viruses, bacteria, and other ligands into cells.

ACKNOWLEDGMENTS

We thank Mary Collins for the GagYFP and Richard E. Pagano for the cav-1 mRed. We also thank Rainer Pepperkok and Jens Rietdorf (AMLF, EMBL Heidelberg) for help with live-cell imaging experiments. Thanks also to Olympus Europa GmbH for their continuous support of the Advanced Light Microscopy Facility at EMBL Heidelberg.

This work was supported by the Lundbeck Foundation, the Novo Nordisk Foundation, the Danish Medical Research Council (grant 22-03-0254), and an Engineer Arne Hansen Grant. C.B. was supported by a grant from the Carlsberg Foundation to L.P. and by the German Academy of Natural Scientists (BMBF-LPD 9901/8-81), using funds from the Bundesministerium für Bildung und Forschung.

REFERENCES

1. **Abramoff, M. D., P. J. Magelhaes, and S. J. Ram.** 2004. Image processing with ImageJ. Biophotonics Int. **11:**36–42.
2. **Anderson, H. A., Y. Chen, and L. C. Norkin.** 1996. Bound simian virus 40 translocates to caveolin-enriched membrane domains, and its entry is inhibited by drugs that selectively disrupt caveolae. Mol. Biol. Cell **7:**1825–1834.
3. **Anderson, R. G.** 1998. The caveolae membrane system. Annu. Rev. Biochem. **67:**199–225.
4. **Andrawiss, M., Y. Takeuchi, L. Hewlett, and M. Collins.** 2003. Murine leukemia virus particle assembly quantitated by fluorescence microscopy: role of Gag-Gag interactions and membrane association. J. Virol. **77:**11651–11660.
5. **Beer, C., D. S. Andersen, A. Rojek, and L. Pedersen.** 2005. Caveolae-dependent endocytic entry of amphotropic murine leukemia virus. J. Virol. **79:** 10776–10787.
6. **Carstanjen, D., P. Dutt, and T. Moritz.** 2001. Heparin inhibits retrovirus binding to fibronectin as well as gene transfer on fibronectin fragments. J. Virol. **75:**6218–6222.

7. **Chen, L. B., N. Maitland, P. H. Gallimore, and J. K. McDougall.** 1977. Detection of the large external transformation-sensitive protein on some epithelial cells. Exp. Cell Res. **106:**39–46.
8. **Courtney, H. S., I. Ofek, W. A. Simpson, D. L. Hasty, and E. H. Beachey.** 1986. Binding of *Streptococcus pyogenes* to soluble and insoluble fibronectin. Infect. Immun. **53:**454–459.
9. **Crouch, E., G. Balian, K. Holbrook, D. Duksin, and P. Bornstein.** 1978. Amniotic fluid fibronectin. Characterization and synthesis by cells in culture. J. Cell Biol. **78:**701–715.
10. **Eash, S., W. Querbes, and W. J. Atwood.** 2004. Infection of Vero cells by BK virus is dependent on caveolae. J. Virol. **78:**11583–11590.
11. **George, E. L., E. N. Georges-Labouesse, R. S. Patel-King, H. Rayburn, and R. O. Hynes.** 1993. Defects in mesoderm, neural tube and vascular development in mouse embryos lacking fibronectin. Development **119:**1079–1091.
12. **Greco, G., S. Pal, R. Pasqualini, and L. M. Schnapp.** 2002. Matrix fibronectin increases HIV stability and infectivity. J. Immunol. **168:**5722–5729.
13. **Hanenberg, H., X. L. Xiao, D. Dilloo, K. Hashimoto, I. Kato, and D. A. Williams.** 1996. Colocalization of retrovirus and target cells on specific fibronectin fragments increases genetic transduction of mammalian cells. Nat. Med. **2:**876–882.
14. **Hedman, K., A. Vaheri, and J. Wartiovaara.** 1978. External fibronectin of cultured human fibroblasts is predominantly a matrix protein. J. Cell Biol. **76:**748–760.
15. **Hynes, R. O.** 1990. Fibronectins. Springer-Verlag, Berlin, Germany.
16. **Julkunen, I., A. Hautanen, and J. Keski-Oja.** 1983. Interaction of viral envelope glycoproteins with fibronectin. Infect. Immun. **40:**876–881.
17. **Kavanaugh, M. P., D. G. Miller, W. Zhang, W. Law, S. L. Kozak, D. Kabat, and A. D. Miller.** 1994. Cell-surface receptors for gibbon ape leukemia virus and amphotropic murine retrovirus are inducible sodium-dependent phosphate symporters. Proc. Natl. Acad. Sci. USA **91:**7071–7075.
18. **Kizhatil, K., and L. M. Albritton.** 1997. Requirements for different components of the host cell cytoskeleton distinguish ecotropic murine leukemia virus entry via endocytosis from entry via surface fusion. J. Virol. **71:**7145–7156.
19. **Klein, R. M., M. Zheng, A. Ambesi, L. Van De Water, and P. J. McKeown-Longo.** 2003. Stimulation of extracellular matrix remodeling by the first type III repeat in fibronectin. J. Cell Sci. **116:**4663–4674.
20. **Kornblihtt, A. R., C. G. Pesce, C. R. Alonso, P. Cramer, A. Srebrow, S. Werbajh, and A. F. Muro.** 1996. The fibronectin gene as a model for splicing and transcription studies. FASEB J. **10:**248–257.
21. **Kühlcke, K., B. Fehse, A. Schilz, S. Loges, C. Lindemann, F. Ayuk, F. Lehmann, N. Stute, A. A. Fauser, A. R. Zander, and H. G. Eckert.** 2002. Highly efficient retroviral gene transfer based on centrifugation-mediated vector preloading of tissue culture vessels. Mol. Ther. **5:**473–478.
22. **Kuusela, P.** 1978. Fibronectin binds to Staphylococcus aureus. Nature **276:** 718–720.
23. **Lei, P., j. B. Baja, and S. T. Andreadis.** 2002. Retrovirus-associated heparan sulfate mediates immobilization and gene transfer on recombinant fibronectin. J. Virol. **76:**8722–8728.
24. **Lin, W., S. M. Wang, T. F. Huang, and W. M. Fu.** 2002. Differential regulation of fibronectin fibrillogenesis by protein kinases A and C. Connect. Tissue Res. **43:**22–31.
25. **Lu, X., and J. Silver.** 2000. Ecotropic murine leukemia virus receptor is physically associated with caveolin and membrane rafts. Virology **276:**251–258.
26. **Mao, Y., and J. E. Schwarzbauer.** 2005. Fibronectin fibrillogenesis, a cell-mediated matrix assembly process. Matrix Biol. **24:**389–399.
27. **Marjomäki, V., V. Pietiäinen, H. Matilainen, P. Upla, J. Ivaska, L. Nissinen, H. Reunanen, P. Huttunen, T. Hyypiä, and J. Heino.** 2002. Internalization of echovirus 1 in caveolae. J. Virol. **76:**1856–1865.
28. **Miller, A. D., and F. Chen.** 1996. Retrovirus packaging cells based on 10A1 murine leukemia virus for production of vectors that use multiple receptors for cell entry. J. Virol. **70:**5564–5571.
29. **Miller, D. G., R. H. Edwards, and A. D. Miller.** 1994. Cloning of the cellular receptor for amphotropic murine retroviruses reveals homology to that for gibbon ape leukemia virus. Proc. Natl. Acad. Sci. USA **91:**78–82.
30. **Molinari, G., S. R. Talay, P. Valentin-Weigand, M. Rohde, and G. S. Chhatwal.** 1997. The fibronectin-binding protein of *Streptococcus pyogenes*, SfbI, is involved in the internalization of group A streptococci by epithelial cells. Infect. Immun. **65:**1357–1363.
31. **Moritz, T., P. Dutt, X. Xiao, D. Carstanjen, T. Vik, H. Hanenberg, and D. A. Williams.** 1996. Fibronectin improves transduction of reconstituting hematopoietic stem cells by retroviral vectors: evidence of direct viral binding to chymotryptic carboxy-terminal fragments. Blood **88:**855–862.
32. **Moritz, T., V. P. Patel, and D. A. Williams.** 1994. Bone marrow extracellular matrix molecules improve gene transfer into human hematopoietic cells via retroviral vectors. J. Clin. Investig. **93:**1451–1457.
33. **Morla, A., Z. Zhang, and E. Ruoslahti.** 1994. Superfibronectin is a functionally distinct form of fibronectin. Nature **367:**193–196.
34. **Nomura, R., A. Kiyota, E. Suzaki, K. Kataoka, Y. Ohe, K. Miyamoto, T. Senda, and T. Fujimoto.** 2004. Human coronavirus 229E binds to CD13 in rafts and enters the cell through caveolae. J. Virol. **78:**8701–8708.
35. **Nunes-Correia, I., A. Eulalio, S. Nir, and M. C. Pedroso de Lima.** 2004. Caveolae as an additional route for influenza virus endocytosis in MDCK cells. Cell. Mol. Biol. Lett. **9:**47–60.
36. **Pankov, R., and K. M. Yamada.** 2002. Fibronectin at a glance. J. Cell Sci. **115:**3861–3863.
37. **Pedersen, L., S. V. Johann, M. van Zeijl, F. S. Pedersen, and B. O'Hara.** 1995. Chimeras of receptors for gibbon ape leukemia virus/feline leukemia virus B and amphotropic murine leukemia virus reveal different modes of receptor recognition by retrovirus. J. Virol. **69:**2401–2405.
38. **Pelkmans, L., J. Kartenbeck, and A. Helenius.** 2001. Caveolar endocytosis of simian virus 40 reveals a new two-step vesicular-transport pathway to the ER. Nat. Cell Biol. **3:**473–483.
39. **Pilka, E. S., J. M. Werner, U. Schwarz-Linek, A. R. Pickford, N. A. Meenan, I. D. Campbell, and J. R. Potts.** 2006. Structural insight into binding of *Staphylococcus aureus* to human fibronectin. FEBS Lett. **580:**273–277.
40. **Pizzato, M., S. A. Marlow, E. D. Blair, and Y. Takeuchi.** 1999. Initial binding of murine leukemia virus particles to cells does not require specific Env-receptor interaction. J. Virol. **73:**8599–8611.
41. **Rohde, M., E. Muller, G. S. Chhatwal, and S. R. Talay.** 2003. Host cell caveolae act as an entry-port for group A streptococci. Cell. Microbiol. **5:**323–342.
42. **Schlessinger, J., L. S. Barak, G. G. Hammes, K. M. Yamada, I. Pastan, W. W. Webb, and E. L. Elson.** 1977. Mobility and distribution of a cell surface glycoprotein and its interaction with other membrane components. Proc. Natl. Acad. Sci. USA **74:**2909–2913.
43. **Sharma, D. K., J. C. Brown, A. Choudhury, T. E. Peterson, E. Holicky, D. L. Marks, R. Simari, R. G. Parton, and R. E. Pagano.** 2004. Selective stimulation of caveolar endocytosis by glycosphingolipids and cholesterol. Mol. Biol. Cell **15:**3114–3122.
44. **Soneoka, Y., P. M. Cannon, E. E. Ramsdale, J. C. Griffiths, G. Romano, S. M. Kingsman, and A. J. Kingsman.** 1995. A transient three-plasmid expression system for the production of high titer retroviral vectors. Nucleic Acids Res. **23:**628–633.
45. **Sottile, J., and J. Chandler.** 2005. Fibronectin matrix turnover occurs through a caveolin-1-dependent process. Mol. Biol. Cell **16:**757–768.
46. **Sottile, J., and D. C. Hocking.** 2002. Fibronectin polymerization regulates the composition and stability of extracellular matrix fibrils and cell-matrix adhesions. Mol. Biol. Cell **13:**3546–3559.
47. **Stenman, S., and A. Vaheri.** 1978. Distribution of a major connective tissue protein, fibronectin, in normal human tissues. J. Exp. Med. **147:**1054–1064.
48. **Uckert, W., G. Willimsky, F. S. Pedersen, T. Blankenstein, and L. Pedersen.** 1998. RNA levels of human retrovirus receptors Pit1 and Pit2 do not correlate with infectibility by three retroviral vector pseudotypes. Hum. Gene Ther. **9:**2619–2627.
49. **Vaheri, A., E. Ruoslahti, B. Westermark, and J. Ponten.** 1976. A common cell-type specific surface antigen in cultured human glial cells and fibroblasts: loss in malignant cells. J. Exp. Med. **143:**64–72.
50. **van Zeijl, M., S. V. Johann, E. Closs, J. Cunningham, R. Eddy, T. B. Shows, and B. O'Hara.** 1994. A human amphotropic retrovirus receptor is a second member of the gibbon ape leukemia virus receptor family. Proc. Natl. Acad. Sci. USA **91:**1168–1172.
51. **Wagner, D. D., and R. O. Hynes.** 1979. Domain structure of fibronectin and its relation to function. Disulfides and sulfhydryl groups. J. Biol. Chem. **254:**6746–6754.
52. **Walker, S. J., M. Pizzato, Y. Takeuchi, and S. Devereaux.** 2002. Heparin binds to murine leukemia virus and inhibits Env-independent attachment and infection. J. Virol. **76:**6909–6918.
53. **Yamada, K. M.** 1978. Immunological characterization of a major transformation-sensitive fibroblast cell surface glycoprotein. Localization, redistribution, and role in cell shape. J. Cell Biol. **78:**520–541.
54. **Yamada, K. M., and K. Olden.** 1978. Fibronectins—adhesive glycoproteins of cell surface and blood. Nature **275:**179–184.
55. **Yamada, K. M., and J. A. Weston.** 1974. Isolation of a major cell surface glycoprotein from fibroblasts. Proc. Natl. Acad. Sci. USA **71:**3492–3496.
56. **Yamada, K. M., S. S. Yamada, and I. Pastan.** 1977. Quantitation of a transformation-sensitive, adhesive cell surface glycoprotein. Decrease of several untransformed permanent cell lines. J. Cell Biol. **74:**649–654.